Materials Research Proceedings 28 (2023) 1387-1396 https://doi.org/10.21741/9781644902479-150

Nonlinear elastic stress triaxiality dependent constitutive model for fibre-reinforced polymer composites

OBID Štefan[1,a], HALILOVIČ Miroslav[1,b] and STARMAN Bojan[1,c *]

[1]University of Ljubljana, Faculty of Mechanical Engineering, Aškerčeva 6, 1000 Ljubljana, Slovenia

[a]stefan.obid@fs.uni-lj.si, [b]miroslav.halilovic@fs.uni-lj.si, [c]bojan.starman@fs.uni-lj.si

Keywords: Constitutive Model, Stress Triaxiality Dependency, Anisotropic Material

Abstract. A novel constitutive model is proposed to describe fibre-reinforced polymer composite materials. The model covers three fundamental phenomena of such materials: anisotropy, tension-compression asymmetry, and nonlinear material behaviour. The model is based on the one-dimensional Ramberg-Osgood relation, which is extended to a multiaxial anisotropic form. Tension-compression asymmetry is then implemented with the introduction of stress triaxiality dependency. Finally, the model is verified using experimental data where the material response in uniaxial tension, uniaxial compression and shear stress states were measured.

Introduction

Fibre-reinforced polymer composites are increasingly used in many manufacturing fields due to their high strength-to-weight ratio and low cost. Their main property is an anisotropic material response which is a consequence of reinforcement fibres orientation. Another essential property caused by reinforcement fibres is tension-compression asymmetry. In tension loading, fibres stretch and increase overall material stiffness, which is not the case in compression loading, where they can buckle due to matrix porosity [1]. The third important property is a nonlinear material response which is mainly a consequence of the polymer matrix and can be observed even at low strains [2]. All three properties must be addressed to accurately model the material response of fibre-reinforced materials.

One of the first attempts at modelling 2D orthotropic material with tension-compression asymmetry was proposed in [3], where different values of compliance tensor components were prescribed depending on the sign of stress tensor components. The problem with this model was thermodynamical inconsistency due to asymmetric compliance tensor, which was later solved in [4] and [5]. Similar variations of tension-compression asymmetry modelling with sign manipulation can be found in [6,7] and later in [8], where this idea was generalised to a 3D constitutive model. Recently, 3D tension-compression asymmetric damage model for fibre-reinforced materials was introduced in [9], where the damage initiation criterion is defined based on a sign of individual stress components or a sign of two stress components sum. For modelling nonlinear material response in large deformations, the hyperelastic approach was used in [10,11], where asymmetry was implemented with the dependency of constitutive parameters based on signs of principal strain or main stress components. Another approach for modelling material asymmetry was introduced in [12,13], where stress triaxiality dependency was implemented in a linear anisotropic model with an additional term to model polymer matrix nonlinear response.

As seen from the literature, there is no unified approach to model the phenomena mentioned above. In the following, we present a novel elastic constitutive model based on the Ramberg-Osgood relation [14], which is extended to a multiaxial anisotropic model. To implement asymmetric material response new approach is used, where constitutive relation consists of two parts defining material response in tension and compression separately. The two parts are weighted

depending on the value of stress triaxiality, which serves as a tension-compression indicator. In this paper, the derivation of the model is shown, including verification based on experimental data.

Derivation of constitutive relation

The derivation of constitutive relation consists of two parts. In the first part, we take the Ramberg-Osgood nonlinear relation and generalise it to obtain a nonlinear anisotropic model. In the second part, we introduce the dependency of stress triaxiality to implement asymmetric material response.

Nonlinear anisotropy.

To ensure thermodynamic consistency, the strain energy function of the developed model must remain a potential function. Therefore, rather than generalising the Ramberg-Osgood relation itself, we generalise its strain energy potential, which we can write as

$$C = \frac{\sigma^2}{2G} + \frac{\zeta^{n+1}}{n+1}\frac{\sigma^2}{K} \tag{1}$$

where σ is stress, G is shear modulus, K is secant modulus, ζ is stress invariant defined as $\sqrt{(\sigma/K)^2}$ and n is an exponent. As stated, we generalise Eq. 1 to multiaxial anisotropic form as

$$C = \frac{1}{2}\boldsymbol{\sigma}:\mathbb{S}:\boldsymbol{\sigma} + \frac{\zeta^{n-1}}{n+1}\boldsymbol{\sigma}:\mathbb{N}:\boldsymbol{\sigma} \tag{2}$$

where $\boldsymbol{\sigma}$ represents the stress tensor, $\mathbb{S}$ linear compliance tensor and $\mathbb{N}$ nonlinear compliance tensor. From the comparison of Eq. 1 and Eq. 2, we can see that linear compliance tensor $\mathbb{S}$ takes the role of shear modulus G, and nonlinear compliance tensor $\mathbb{N}$ takes the role of secant modulus. Stress invariant ζ is generalised in a similar manner to $\sqrt{\boldsymbol{\sigma}:\mathbb{N}:\mathbb{N}:\boldsymbol{\sigma}}$. With derivation of expression Eq. 2 with respect to stress tensor, we obtain nonlinear anisotropic constitutive relation

$$\boldsymbol{\varepsilon} = \frac{\partial C}{\partial \boldsymbol{\sigma}} = \mathbb{S}:\boldsymbol{\sigma} + \frac{\zeta^{n-1}}{n+1}\left((n-1)\frac{\boldsymbol{\sigma}:\mathbb{N}:\boldsymbol{\sigma}}{\zeta^2}\mathbb{N} + 2\mathbb{I}^{sym}\right):\mathbb{N}:\boldsymbol{\sigma} \tag{3}$$

where $\mathbb{I}^{sym}$ represents 4-th order symmetric identity.

Tension-compression asymmetry.

The dependency of stress triaxiality is used to implement asymmetric material response. Stress triaxiality η is stress invariant defined as the ratio between hydrostatic pressure p and von Mises stress q

$$\eta = -\frac{p}{q} \tag{4}$$

The absolute value of stress triaxiality indicates how uniform is stress state distributed between three material axes. The crucial property for implementing asymmetric behaviour is the stress triaxiality sign, which is positive in tensile stress states, and negative in compressive stress states. We can now define strain energy as a function of stress triaxiality as

$$\mathrm{C} = \mathrm{C_t}\,\psi_t(\eta) + C_c\,\psi_c(\eta) \tag{5}$$

where C_t and C_c are tensile and compressive strain energy functions defined the same as Eq. 2, where separate tensors $\mathbb{S}$, $\mathbb{N}$ and exponent n are assigned to each one. Both parts of Eq. 5 contain weight functions $\psi_t(\eta)$ or $\psi_c(\eta)$ which are piecewise defined, as shown in Fig. 1.

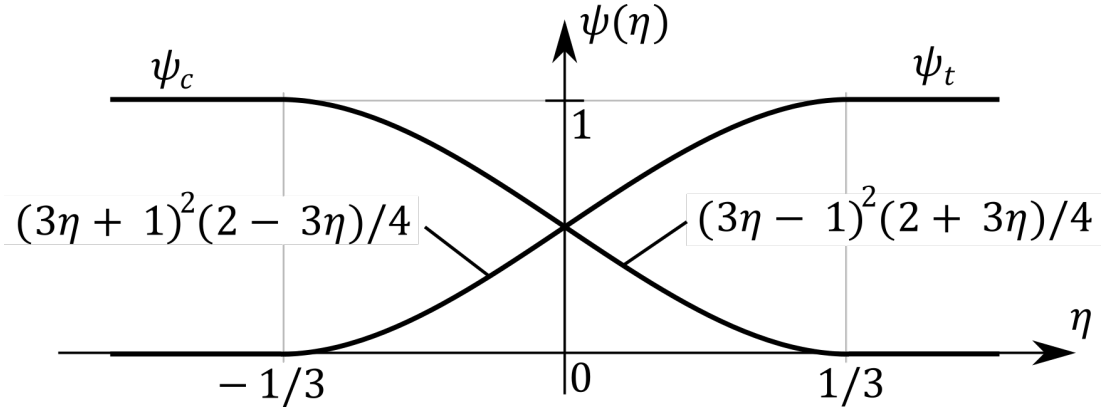

Fig. 1. Weight functions $\psi_t(\eta)$ and $\psi_c(\eta)$.

With such defined weight functions energy part C_t only affect material behaviour in tensile stress states and vice versa, C_c only has an effect in compressive stress states. In the transition zone between uniaxial compression ($\eta = -1/3$) and uniaxial tension stress state ($\eta = 1/3$), where both energy parts are intertwined, the weight functions are defined as a third-order polynomial.

Taking the derivative of strain energy density (Eq. 5) with respect to stress tensor yields final constitutive relation, which in shortened form can be written as

$$\boldsymbol{\varepsilon} = \left(\frac{\mathrm{d}\psi_t(\eta)}{\mathrm{d}\eta} C_t + \frac{\mathrm{d}\psi_c(\eta)}{\mathrm{d}\eta} C_c\right)\frac{\partial \eta}{\partial \boldsymbol{\sigma}} + \psi_t(\eta)\frac{\partial C_t}{\partial \boldsymbol{\sigma}} + \psi_c(\eta)\frac{\partial C_c}{\partial \boldsymbol{\sigma}} \tag{6}$$

Constitutive relation (Eq. 6) is valid for general nonlinear anisotropic and asymmetric material. If no tension-compression asymmetry is observed, the relation simplifies to Eq. 3. Furthermore, if material behaviour is linear, the model reduces to classic linear anisotropic form written as

$$\boldsymbol{\varepsilon} = \mathbb{S} : \boldsymbol{\sigma} \tag{7}$$

Compliance Tensor Structure

In this section, the compliance tensor structure and containing parameters are shown. For simplicity sake, we will restrict from general anisotropy to orthotropic material. In this case, linear compliance tensors $\mathbb{S}_t$ and $\mathbb{S}_c$ take the following form in Voigt notation

$$[\mathbb{S}_\alpha] = \begin{bmatrix} 1/E_1^\alpha & -\nu_{12}^\alpha/E_1^\alpha & -\nu_{13}^\alpha/E_1^\alpha & 0 & 0 & 0 \\ -\nu_{12}^\alpha/E_1^\alpha & 1/E_2^\alpha & -\nu_{23}^\alpha/E_2^\alpha & 0 & 0 & 0 \\ -\nu_{13}^\alpha/E_1^\alpha & -\nu_{23}^\alpha/E_2^\alpha & 1/E_3^\alpha & 0 & 0 & 0 \\ 0 & 0 & 0 & 1/G_{12}^\alpha & 0 & 0 \\ 0 & 0 & 0 & 0 & 1/G_{13}^\alpha & 0 \\ 0 & 0 & 0 & 0 & 0 & 1/G_{23}^\alpha \end{bmatrix}, \quad \alpha \in \{t, c\} \tag{8}$$

where E_i^α is an elastic modulus, G_{ij}^α is a shear modulus and ν_{ij}^α is a Poisson's ratio. Nonlinear compliance tensors $\mathbb{N}_t$ and $\mathbb{N}_c$ have a similar form to linear compliance tensors and are formulated as

Materials Research Proceedings 28 (2023) 1387-1396 https://doi.org/10.21741/9781644902479-150

$$[\mathbb{N}_\alpha] = \begin{bmatrix} 1/A_{11}^\alpha & 1/A_{12}^\alpha & 1/A_{13}^\alpha & 0 & 0 & 0 \\ 1/A_{12}^\alpha & 1/A_{22}^\alpha & 1/A_{23}^\alpha & 0 & 0 & 0 \\ 1/A_{13}^\alpha & 1/A_{23}^\alpha & 1/A_{33}^\alpha & 0 & 0 & 0 \\ 0 & 0 & 0 & 1/B_{12}^\alpha & 0 & 0 \\ 0 & 0 & 0 & 0 & 1/B_{13}^\alpha & 0 \\ 0 & 0 & 0 & 0 & 0 & 1/B_{23}^\alpha \end{bmatrix}, \quad \alpha \in \{t, c\} \tag{9}$$

where A_{ij}^α and B_{12}^α are parameters defining nonlinear material response. We can see that linear compliance tensors contain well-known parameters for describing linear elastic properties, whereas, in nonlinear compliance tensors, parameters have no direct physical meaning.

Parameter Identification Procedure

The derived constitutive model (Eq. 6) has four compliance tensors $\mathbb{S}_t$, $\mathbb{N}_t$, $\mathbb{S}_c$, $\mathbb{N}_c$ and two exponents n_t, and n_c. Each parameter dictates a particular part of the model response (see Table 1).

Table 1. Parameter influence on the model response.

model response	*compressive*	*tensile*
linear	$\mathbb{S}_c$	$\mathbb{S}_t$
nonlinear	$\mathbb{N}_c, n_c$	$\mathbb{N}_t, n_t$

This property enables parameters to be separately identified in four groups, as indicated in Table 1. Identification procedure is performed in the following steps:

1) Uniaxial tensile tests are used, from which linear tensile parameters are identified based on initial slopes of strain-stress curves, yielding a linear system of equations from which parameter values are calculated.
2) With linear parameters known, we can proceed to nonlinear parameter identification. The same test set is used in the first step, whereas whole strain-stress curves are now used, not just initial slopes. In this step, parameters cannot be directly calculated. Therefore, optimisation methods are used to minimise the deviation between model response and experimental data. In our case, the procedure is carried out in Wolfram Mathematica software by applying the BFGS quasi-Newton method to a scatter of points randomly distributed over the parametric hyperspace.
3) 1. and 2. steps are repeated where compressive linear and nonlinear parameters are identified based on uniaxial compression tests.

Fig. 2 shows which part of the material response and which model parameters are determined in which identification step.

Materials Research Proceedings 28 (2023) 1387-1396 https://doi.org/10.21741/9781644902479-150

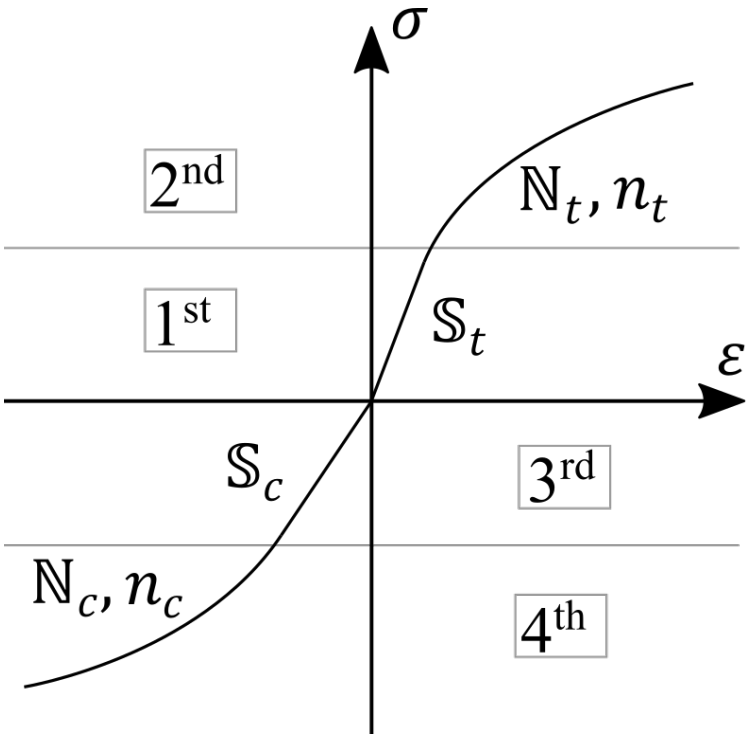

Fig. 2. Four-step identification procedure.

In each step, uniaxial tests performed in different material orientations are used to identify all parameters in compliance tensors. The choice of specimen orientations is identical as in the identification of classic linear anisotropic or orthotropic material.

Validation

To validate the developed model, we used the material properties of a unidirectional glass-fibre epoxy composite carried out in [1]. In this study, besides linear orthotropic properties, tension-compression asymmetry of elastic moduli and nonlinear material response in an off-axis direction were also determined. The nonlinear material response was separately described with three parametric Ramberg-Osgood relation

$$\gamma_{ij} = \frac{\sigma_{ij}}{G_{ij}} + \left(\frac{\sigma_{ij}}{K_{ij}}\right)^{1/N_{ij}}, \qquad \text{ij} \in \{12, 13, 23\} \tag{10}$$

Material properties determined in [1] which have the same values in tension and compression, are listed in Table 2, and elastic moduli are separately listed in Table 3.

Table 2. Material properties from [1].

ij	12	13	23
ν_{ij}^{α}[/]	0.29	0.27	0.41
G_{ij}^{α}[GPa]	4.25	4.16	4.47
K_{ij}^{α}[MPa]	211	191	∞
N_{ij}^{α}[/]	0.237	0.219	/

$\alpha \in \{t, c\}$

Materials Research Proceedings 28 (2023) 1387-1396 https://doi.org/10.21741/9781644902479-150

Table 3. Elastic moduli from [1].

α	t	c
E_1^α[GPa]	49.1	47.9
E_2^α[GPa]	12.8	12.5

These experimental data are useful for validating the developed model because of its ability to describe all fundamental phenomena of this material behaviour, namely, orthotropy, nonlinearity and asymmetry. Since our model also use classic parameters for the description of linear material response, values from Table 2 and Table 3 can be directly used to determine linear compliance tensors $\mathbb{S}_t$ and $\mathbb{S}_c$. Since our model is also based on the Ramberg-Osgood relation, one would expect that nonlinear properties $\mathbb{N}_\alpha$ and n_α will be directly computed from K_{ij}^α and N_{ij}^α from Table 2, which is not the case. The reason is the exponent N_{ij}^α, which has different values in different directions, not alike in our model, which has the same value of the exponent n_α for all material directions. Therefore, nonlinear properties have to be determined using optimisation and are listed in Table 4.

Table 4. Optimised values of nonlinear parameters.

A_{ij}^α[MPa]$\star$	B_{12}^α[MPa]	B_{13}^α[MPa]	B_{23}^α[MPa]	n^α [/]
∞	154.3	151.5	∞	4.404

$\alpha \in \{t, c\}, \quad \star\, i, j \in \{1, 2, 3\}$

To validate the developed model properly, we compared the 3-point bending test finite element simulation results carried out in [1] and the simulation done with our constitutive model, which was implemented in the Abaqus finite element software via the VUMAT subroutine. Fig. 3 shows the comparison of both simulation results. Since the bending test is symmetrical, only half of the field is shown in the figure with symmetry plane on the left side. The compared strain fields are almost identical, where only a minuscule difference can be observed in the shear strain field.

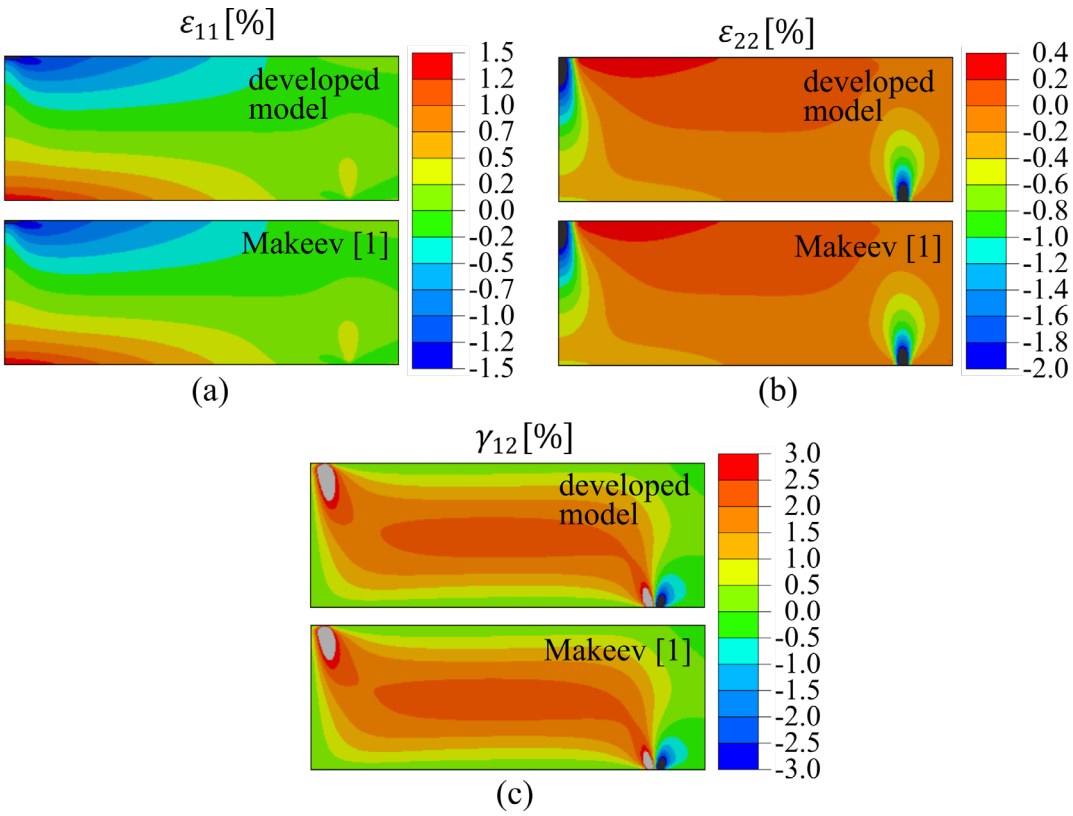

Fig. 3. Comparison of 3-point bending FEM simulation results.

Verification

In this section, verification of the developed model is presented. Redundant experimental data set is used, where more data are available than needed for model calibration, which enables us to verify whether the model prediction agrees with the rest of the experimental data, which were not used for calibration.

Experimental data used for verification were carried out in [15], where multiple in-plane tests were performed for woven roving glass fibre composite plates. Specimens were cut from the plate at 0°, 22.5° and 45° angles with respect to fibre orientation. For each direction, uniaxial tension, uniaxial compression and shear tests were performed, where longitudinal and transversal strains were measured. In total, 9 tests and 18 strain-stress curves were carried out (shown in Fig. 4).

For model calibration, only tension and compression tests in 0° and 45° directions are used, which is 4 out of 9 tests. With four step identification procedure, the parameter values in Table 5 were determined.

Table 5. Calibrated values of model parameters from experimental data.

α	E_1^α [GPa]	E_2^α [GPa]	G_{12}^α [GPa]	ν_{12}^α [/]	A_{11}^α [GPa]	A_{22}^α [GPa]	A_{12}^α [GPa]	B_{12}^α [GPa]	n_α [/]
t	19.8	14.2	4.86	0.152	1.69	174	7.46	0.223	2.43
c	18.2	13.1	4.15	0.199	∞	1.77	-2.27	0.130	3.57

A comparison of experimental curves and model response is shown in Fig. 4, where columns represent different material orientations, and rows represent different loading cases.

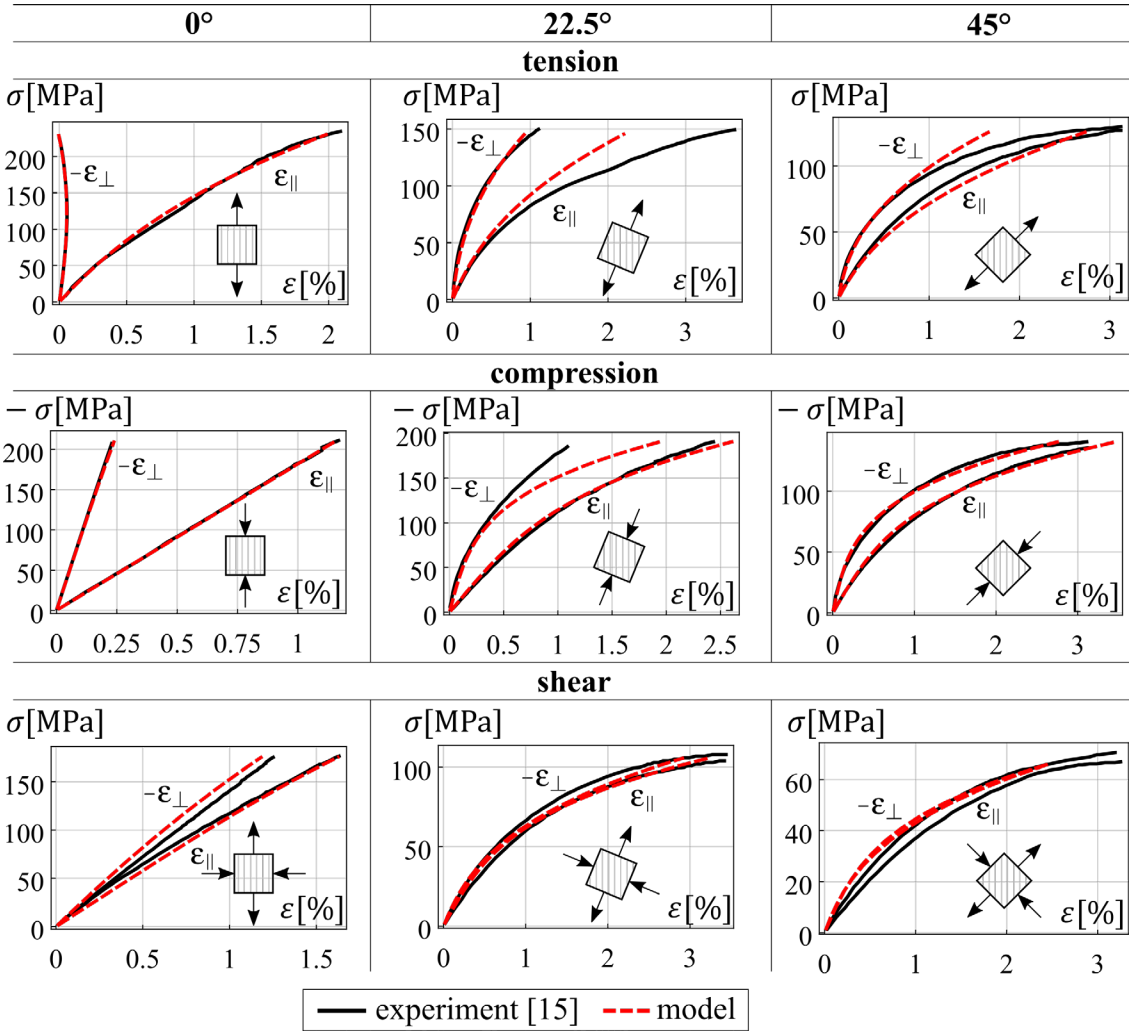

Fig. 4. Comparison of experimental and model strain-stress curves.

For a more quantitative comparison, an absolute relative error between experimental data and model response strain energy density was calculated using the equation below

$$err = \left|\frac{C_{model} - C_{exp}}{C_{exp}}\right| \cdot 100\% \tag{11}$$

where model strain energy C_{model} is calculated by equation (5), and experimental strain energy C_{exp} is calculated as the area under the stress-strain diagram. Calculated error values represent a relative difference in the area below the model and experimental curves. The calculated values are specified in Table 6.

Table 6. Calculated relative error for each loading case.

relative error *err* [%]	0°		22.5°		45°	
	∥	⊥	∥	⊥	∥	⊥
tension	0.721	1.537	10.914	0.687	3.766	3.813
compression	0.424	1.874	0.005	18.353	0.052	0.447
shear	20.950	25.367	4.183	5.907	8.618	2.670

It is not surprising that model responses show good agreement with experimental curves from which the model was calibrated (colored green in Table 6), where maximal error is 3.766%. Values, colored yellow in Table 6, represent relative error in loading cases which were not included in the calibration procedure. High error values in some responses could be lowered with inclusion of all experimental data in calibration procedure. However, ideally one would want to capture material behaviour from as few experiments as possible. Therefore, it is more important to see that model can correctly predict material behaviour from just uniaxial tension and compression test in two different orientations.

Summary

The novel constitutive model for the description of anisotropic, nonlinear and asymmetric material behaviour was presented. The nonlinear Ramberg-Osgood relation was generalised to an anisotropic form, where stress triaxiality dependency was introduced to achieve tension-compression asymmetry.

Quite a few parameters are needed to capture all the phenomena mentioned above, which are identified in separate groups in a four-stage identification procedure. The model uses classic linear anisotropic parameters to describe the linear part of the model response, which is convenient when values of those parameters are already given. Another good property of the model is that it reduces to a simpler form or, ultimately, to a linear anisotropic model if the material does not exhibit all the aforementioned phenomena. In that case, also the number of parameters is drastically decreased.

A redundant experimental data set was used for verification, where good prediction properties of the model were shown. The model was able to predict a comparable response to experimental data in a 22.5° direction and in a shear stress state, both of which were not included in the calibration procedure.

References

[1] E.V. Lomakin, Y.N. Rabotnov, A theory of elasticity for an isotropic body with different moduli in tension and compression, Mech. Solid. 13 (1978) 25-30.

[2] Y. He, A. Makeev, Nonlinear shear behavior and interlaminar shear strength of unidirectional polymer matrix composites: A numerical study, Int. J. Solid. Struct. 51 (2014) 1263-1273. https://doi.org/10.1016/j.ijsolstr.2013.12.014

[3] S.A. Ambartsumian, A.A. Khachatrian, Basic equations in the theory of elasticity for materials with different resistance to tension and compression, Inzhenernyi zhurnal – Mekhanika tverdogo tela (1966) 44–53.

[4] R.M. Jones, Stress-strain relations for materials with different moduli in tension and compression, Aiaa J. 15 (1977) 16-23.

[5] C.W. Bert, Models for fibrous composites with different properties in tension and compression, J. Eng. Mater. Technol. 99 (1977) 344-349. https://doi.org/10.1115/1.3443550

[6] B.P. Patel, K. Khan, Y. Nath, A new constitutive model for bimodular laminated structures: Application to free vibrations of conical/cylindrical panels, Compos. Struct. 110 (2014) 183-191. https://doi.org/10.1016/j.compstruct.2013.11.008

[7] K. Vijayakumar, K.P. Rao, Stress-strain relations for composites with different stiffnesses in tension and compression, Comput. Mech. 2 (1987) 167-175. https://doi.org/10.1007/BF00571022

[8] L. Zhang, H.W. Zhang, J. Wu, B. Yan, A stabilised complementarity formulation for nonlinear analysis of 3D bimodular materials, Acta Mech. Sin. 32 (2016) 481-490. https://doi.org/10.1007/s10409-015-0517-3

[9] J. Park, J.W. Yoon, A general FRC (fiber reinforced composite) constitutive model considering transverse isotropy and accumulated damage, J. Mech. Sci. Tech. 36 (2022) 6147-6156. https://doi.org/10.1007/s12206-022-1129-z

[10] M. Latorre, F.J. Montáns, Bi-modulus materials consistent with a stored energy function: Theory and numerical implementation, Comput. Struct. 229 (2020) 106176. https://doi.org/10.1016/j.compstruc.2019.106176
[11] Z. Du, G. Zhang, T. Guo, S. Tang, X. Guo, Tension-compression asymmetry at finite strains: A theoretical model and exact solutions, J. Mech. Phys. Solid. 143 (2020) 104084. https://doi.org/10.1016/j.jmps.2020.104084
[12] E.V. Lomakin, B.N. Fedulov, Nonlinear anisotropic elasticity for laminate composites, Meccanica 50 (2015) 1527-1535. https://doi.org/10.1007/s11012-015-0104-5
[13] E.V. Lomakin, O.P. Shchendrigina, Stresses and strains in a disk of physically nonlinear material with stress state dependent properties, Mech. Solid. 55 (2020) 475-481. https://doi.org/10.3103/S0025654420040081
[14] W. Ramberg, W.R. Osgood, Description of stress-strain curves by three parameters, Technical Report NACA-TN-902, 1943.
[15] E.W. Smith, K.J. Pascoe, The role of shear deformation in the fatigue failure of a glass fibre-reinforced composite, Compos. 8 (1977) 237-243.